Available online at www.sciencedirect.com

ScienceDirect

IFAC PapersOnline CONFERENCE PAPER ARCHIVE

IFAC PapersOnLine 58-24 (2024) 151–156

Influence of Changes in Functional Residual Capacity on EIT Imaging in Spontaneous Breathing

M. García Hermosa*, B. Laufer, S. Krueger-Ziolek**, M. Termenon* and K. Moeller****

**Faculty of Engineering (MM-ENG), Mondragon Unibertsitatea, Spain (Tel: +34 681044523; e-mail: maite.ghermosa@gmail.com).*

***Institute of Technical Medicine (ITeM), Furtwangen University, Villingen-Schwenningen, Germany*

Abstract: A deeper understanding of lung ventilation can improve the treatment of patients with lung disease. The aim of this study was to investigate the effects of changes in Functional Residual Capacity (FRC) on electrical impedance tomography images in six healthy, spontaneously breathing subjects. The study involved requesting and analyzing EIT images during tidal breathing at two different FRC levels in a single thoracic plane (5th intercostal space). The differential FRC value (more than 0.5 l) was determined with an optoelectronic plethysmograph, and simultaneously a spirometer was used as a reference system to obtain further respiratory parameters such as tidal volume. Analysis of the spatial distribution of tidal ventilation in the EIT images showed variations in air homogeneity based on the air shift to the central area of the lung with increasing FRC values. Additional knowledge about the air distribution at different FRC levels might improve and support the therapy of lung diseases.

Keywords: Functional residual capacity, spontaneous breathing, electrical impedance tomography, optoelectronic plethysmography, ventilation distribution.

1. INTRODUCTION

The World Health Organization has released its most comprehensive compilation of World Health Statistics up until the year 2019 (World Health Statistics 2023 - A Visual Summary, n.d.). The statistics reveal the extent to which main diseases have affected global health systems, being respiratory disorders the third largest contributor to global mortality. Some of the lung disorders present severe symptoms that could affect the air distribution and breathing flow, that in many cases lead to hospitalization. However, mechanical ventilation can also lead to ventilator-induced lung injury (Berlin, 2012). Especially, as the human lung has a reduced regenerative capacity compared to other organs (Cao & Xiao, 2018; Lucas et al., 2020), any support that can help prevent lung disease or support therapy should be used.

Spirometry is often used to test lung function and to diagnose obstructive lung diseases like chronic obstructive pulmonary disease (COPD) or cystic fibrosis. However, due to the effort required by patients, it is not suitable for all patients. (Hochhausen et al., 2022). To overcome the limitation of spirometry (Zhou & Zhou, 2021), research in the field of lung diagnostics continues (Laufer et al., 2021). As an alternative, multiple studies identified Optoelectronic Plethysmography (OEP) as a suitable approach for assessing lung capacities and movement of the chest wall in individuals across different age groups (Massaroni et al., 2017; Zhou & Zhou, 2021). OEP is a non-invasive system which captures alterations in chest wall dynamics during respiration and models the thoraco-abdominal surface without the need for extra breathing effort.

Other measurement methods such as electrical impedance tomography (EIT) allow the monitoring of regional changes in lung ventilation. EIT measures changes in the impedance of lung tissue by using small electrical currents, so the surface potentials are measured and reconstructed to generate EIT images that reflect the distribution of air in the lungs (Zhou & Zhou, 2021). Currently, some studies had analyzed the influence of air recruitment in EIT images. Most of them have been carried out in ventilated animals and humans with lung diseases, such as COPD (Ambrisko et al., 2016; Yang et al., 2023a, 2023b; Zick et al., 2013). These studies analyzed recruitment of the lung in different positive end-expiratory pressures in anaesthetized and ventilated subjects. The investigations concluded that tidal recruitment can be measured by an EIT-based analysis. However, few of the studies analyzed whether the obtained results were caused by the lung disease or the behavior of air at an increased functional residual capacity (FRC), (Zhang et al., 2018).

Body plethysmography is the most widely method for assessing FRC levels, nonetheless its applicability can be challenging for patients with certain respiratory disorders or health issues, due to the effort required (Zhou & Zhou, 2021). The absolute values of FRC cannot be determined by spirometry or OEP, however an OEP can be used to determine changes in FRC level.

Consequently, this observational study offers a different perspective by examining the effects of FRC changes on EIT images in healthy, spontaneously breathing individuals, thus providing an insight of FRC levels on air distribution in the lungs. Knowledge of the air distribution in the lungs could improve the success of therapy for patients with lung diseases by enabling the targeted administration of medication inside the lungs, and also improve the oxygenation of patients by breathing specifically into lung-healthy areas.

10.1016/j.ifacol.2024.11.028

2. METHODOLOGY

2.1 Measurement system

The measurement system consisted of a system combining EIT (PulmoVista® 500, Dräger, Germany) with OEP motion tracking system (Bonita, VICON, Denver, CO) and a spirometer (SpiroScout®, Ganshorn Medizin Electronic, Germany). The subjects were performing respiratory maneuvers in sitting position, while EIT, spirometer and OEP measured simultaneously, see Figure 1.

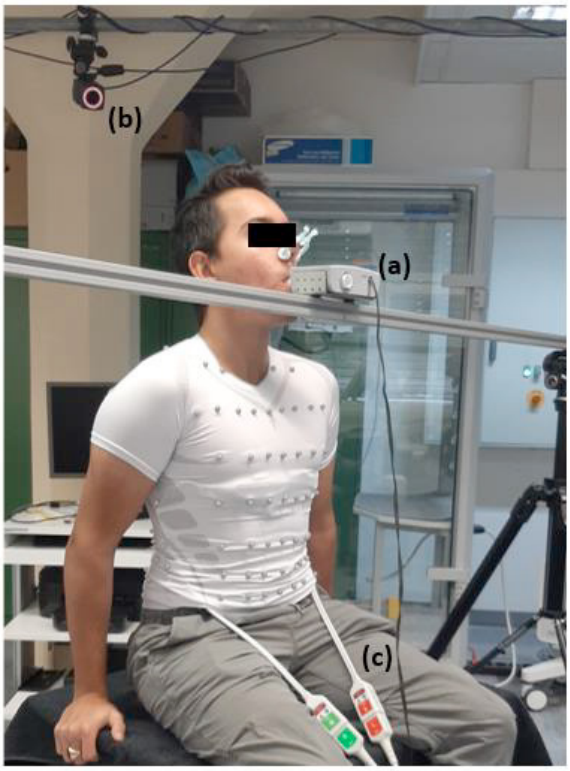

Figure 1. Setup of measurement system combining spirometer, optoelectronic plethysmography with electrical impedance tomography. (a) spirometry unit, (b) optoelectronic plethysmography, and (c) EIT electrode cable feedthrough to the EIT belt on the skin surface.

As illustrated in Figure 2, the EIT measurements were carried out in the mid-axillary line (5th intercostal section (ICS)) of the chest (Krueger-Ziolek et al., 2015). Boundary voltages were collected with an electrode belt of 16 electrodes. A reference electrode was fixed at the subject's abdomen out of the lung area. EIT data was acquired with a frame rate of 40 Hz.

Figure 2.Sketch of the EIT device and the EIT electrode belt in height of ICS5.

The OEP obtained the chest wall motion during the study. Therefore, 102 reflective markers were used, and a 9 infrared camera system (VICON Bonita B10, Firmware Version 404) working at 40 Hz sampling frequency was surrounding the subject. The 102 passive markers were fixed on a compression shirt (Figure 1 and Figure 3) on the anterior and posterior side of the trunk, according to the protocol described by (Laufer et al., 2020).

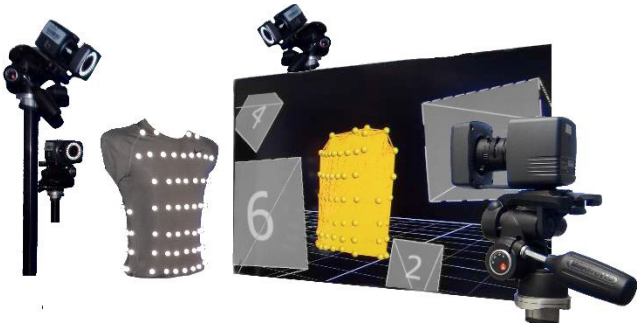

Figure 3. Sketch of the OEP the compression shirt with 102 reflective markers, cameras of the infrared camera system and the illustration of the shirt by the OEP system.

Finally, the spirometer was used to obtain respiration volumes and thus, tidal volumes and to ensure comparable measurements and streamline data analysis during the maneuver. Spirometer data was acquired with a frame rate of 200 Hz.

2.2 Participants

According to the working principles of the measuring devices that are used in this study, subjects with pacemaker or electrical devices have been dismissed. Furthermore, subjects below 18 years and subjects with respiratory disorders are excluded from the study as well as pregnant women. Therefore, the study was performed on six healthy male subjects (weight 74 ± 9.19 kg; height 178 ± 0.04 cm; age 25 ± 4.85 years (mean ± SD)). All subjects gave written, informed consent before they participated in this study.

2.3 Respiratory maneuver

To obtain the required data, measurements were done in two different FRC levels with a minimum difference ΔFRC of 0.5 L. At the same time, to ensure comparable data, only breaths were used for analysis, which had a maximal difference in tidal volumes (TV) of 0.15 L.

Figure 4 illustrates the different phases of the breathing maneuver performed by the subjects. In the first phase, the subject breathed spontaneously for approximately one minute. Afterwards, the FRC levels phase will start with a maximum exhalation, that will be followed by an inhalation of a volume of 1 L. This volume defined the FRC_1. While FRC_1 volume is maintained, the subject inhaled and exhaled 1 L of TV for approximately another minute. Finally, the FRC_2 phase started with a maximal exhalation followed by the inhalation of an FRC of 2 L; similarly, while maintaining this volume, the subject breathed 1 L of TV on top of the FRC for about another minute. The change in FRC is given by:

$$\Delta FRC = FRC_2 - FRC_1 \quad (1)$$

Assistance software was used to enable the subject to see when the desired tidal volume or FRC was reached. This assistance software extracted the required data from the spirometer and was only used to support the subjects; the volume data used for evaluation was obtained directly from the spirometer.

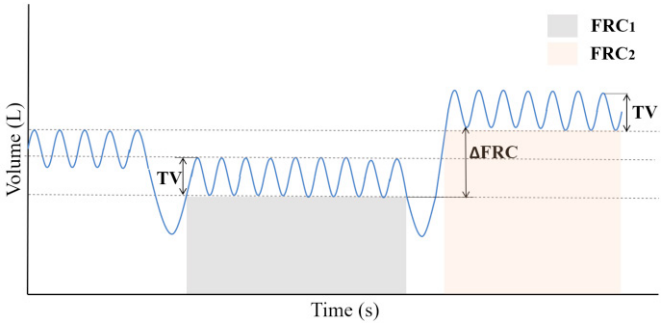

Figure 4. Sketch of the volume curve of the respiratory maneuver performed by the subjects.

2.4 Data reconstruction

The EIT data was reconstructed with a linearized FEM-based Newton-Raphson method using the software supplied by the EIT manufacturer (Dräger EIT Data Analysis Tool 6.3, Dräger, Germany). To isolate the information associated with lung function and reduce cardiac interference, a low-pass filter of 50 min^{-1} was applied. Then the lowest impedance value was defined as baseline.

To minimize the impact of intrathoracic tissues, others than lung tissue, on EIT data, specific regions were defined for each measurement using the following criteria in each FRC level (Krueger-Ziolek et al., 2015). First, compute the difference images between end-inspiration and end-expiration during the normal tidal breathing to depict variations in impedance values. The averaged tidal images within a FRC phase was termed functional EIT image (fEIT). The pixel with the highest value in the fEIT image was determined. Subsequently, pixel values exceeding 20 % of the highest pixel value in the fEIT image were associated with respiration, utilized for further calculations, and defined the region of interest (ROI). The sum of the defined ROIs of the two FRC phases resulted in the creation of a final ROI.

The motion capture based OEP measured the volume of the upper body, enclosed by the reflective markers. Therefore, the 3D shape of the chest wall was generated, and the volume was computed (using MATLAB's *alphaShape* function). Disregarding pressure-related volume variations, the change in volume of the upper body corresponds to the change in FRC.

Finally, spirometry data typically involves measuring airflow, which is then integrated to obtain the corresponding volume. Integrating the airflow often leads to a trend that needs to be removed in order to enhance data interpretation. To remove the trends from the spirometer signals the *detrend* MATLAB function was applied and interpolated to a 40 Hz frequency.

2.5 Data analysis

The EIT data, OEP data and the spirometer data were aligned in time. Afterwards, the difference between the Spirometer's end-inspiration and end-expiration points was calculated to determine the average tidal volume at each FRC level. Subsequently, tidal volumes that did not exceed the averaged values of the tidal volume with a deviation of ± 0.15 L were identified and used for further calculation. Then, the OEP's end-expiratory values (EEV) were used to calculate the average upper body volume for each FRC level. The end-expiratory values of previously labeled data points were grouped into levels and analyzed individually. Those EEV that did not exceed the average EEV values by a deviation of ± 0.18 L were considered for further analysis on the EIT images.

To ensure comparability among EIT images between FRC levels, mean tidal images were generated for each FRC level. Therefore, images of end-expiration were subtracted from images of end-inspiration and averaged (Yang et al., 2021). This was done using the previously identified data points. Four tidal images, with similar FRC and TV values, were used to calculate such a mean tidal EIT image which then was used for further analysis. Figure 5 depicts three areas where ventilation distribution was analyzed: the ventral section at the top, followed by the central section, and finally, the dorsal section at the bottom of the lung. The percentage of air distribution was determined by adding the impedance values of all the pixels of the desired area and divided it by the sum of all pixels within the whole image.

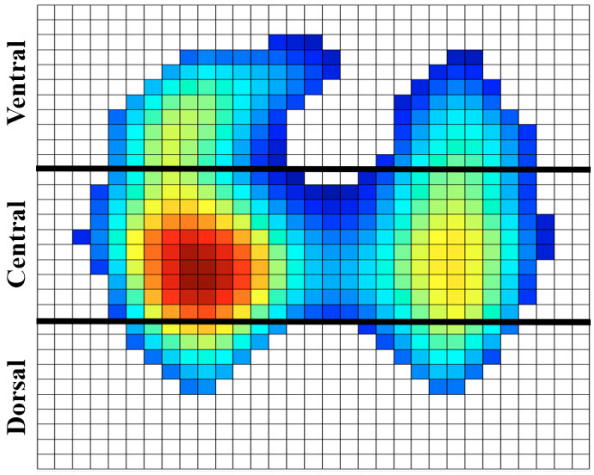

Figure 5. The defined Region of interest for the mean fEIT images. In the upper section of the image the ventral area of the lung, followed by the central area of the lung and the dorsal area. These areas are separated by black lines in the figure.

3. RESULTS

A total of six subjects were included in this study. Figure 6 displays the mean tidal EIT images at two different FRC levels of each subject. The higher FRC level is shown at the left site, whereas the lower FRC level is shown at the right. In addition, under each mean tidal EIT image the percentage of ventilation of the three different regions (ventral, middle and dorsal) are shown.

Regarding spatial distribution, there is a general rise in impedance within the central section for each subject with increasing FRC. It can be noted that approximately 74 ± 4% of lung impedance is located within the central area at high FRC levels compared to the 64 ± 5% at low FRC levels (Mean ± SD). Additionally, it is observed an increase in impedance within the central area between the left and right lung at higher FRC level, across all subjects.

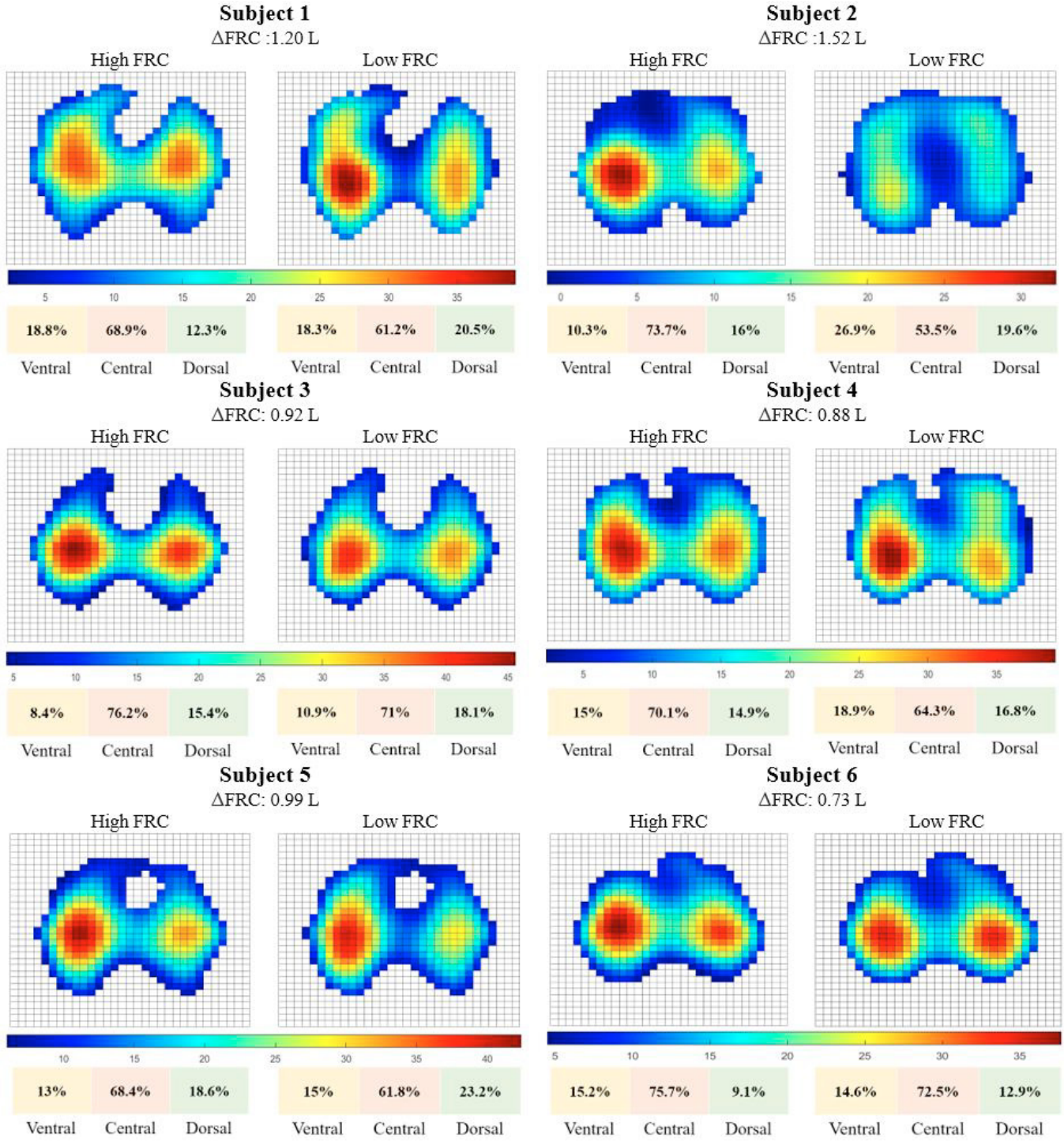

Figure 6. Mean tidal EIT images and percentage of ventilation distribution (ventral, middle and dorsal) within each FRC level of the six subjects. Regarding homogeneity, the smaller the impedance percentage difference between ROI the more homogeneous the air is distributed.

4. DISCUSSION

This preliminary study, combining EIT and OEP measuring techniques provides valuable insights into the understanding of air distribution at different FRC levels. The mean tidal EIT images revealed changes in air distribution as FRC levels increased and it is evident that changes in the FRC levels have an impact on EIT illustration.

If we look at the central parts of the lung, we see an increase in the central ventilation distribution for all subjects as the FRC rises, which is highlighted in red (higher percentages of ventilation distribution) under the EIT images in Figure 6.

In five out of the six cases (subjects 2 to 6), the air is uniformly distributed at lower FRC levels. Compared to that, in subject 1 the air is uniformly distributed at higher levels and tends to increase in the center of the lung as FRC decreases. However, the homogeneity of EIT images is influenced by various reasons. The observed inhomogeneity of high levels could be caused by movement of air from lower parts of the lung towards higher areas (Milic-Emili et al., 1966). On the other hand, it is though that the breathing technique may influence the homogeneity of the air. A study showed that diaphragmatic breathing resulted in more homogeneous breathing than the quiet tidal breathing (Yang et al., 2023c).

Additionally, the results confirmed an increase in the central area of the lung of all subjects with a rising FRC level. This observation should be taken into account during EIT image interpretation e.g. in spontaneously breathing patients with obstructive lung diseases such as COPD who often exhibiting a higher FRC.

The measurements showed that the subjects had difficulties in breathing at a FRC level that deviated from their normal FRC level. The subjects automatically returned to their usual FRC level after a few breaths. It was only possible to maintain the predetermined FRC level for a short time. Therefore, the breaths from the measured data set that were at a comparable FRC level and that differed minimally in tidal volume were used for analysis, as they fulfill the constraints. In particular, the different FRC levels (ΔFRC) should differ by at least 0.5 L and the breaths should have a maximum difference in tidal volume of 0.15 L.

The extent of changes in ventilation distribution could possibly be influenced by variations in ΔFRC, as in the examples of subject 2 with a ΔFRC of 1.52 L and subject 6 with a ΔFRC of only 0.73 L illustrate. Despite all subjects exhibit similar trends, further investigation into the effects of variations in ΔFRC on ventilation distribution is needed. This could involve normalizing the ventilation changes for each individual based on their respective ΔFRC. This study shows that changes in FRC have an influence on EIT imaging. The current study only examined six lung-healthy men of similar age, weight and height. In order to confirm the promising results, a further study with more subjects of different ages, body types and genders should be conducted. This would lead to a deeper understanding of how FRC affects air distribution in the lungs.

A deeper understanding of air distribution in the lungs could improve the success of therapy for people with lung disease, as it could be used for more targeted drug administration or to improve oxygenation in damaged lungs.

5. CONCLUSIONS

The results obtained showed the influence of changes in functional residual capacity on the distribution of air in the lung and thus, on EIT imaging. These effects could enhance lung therapies by targeted drug administration in the lungs.

ACKNOWLEDGEMENT

This work was partially supported by the German Federal Ministry for Economic Affairs and Climate Action (BMWi) (ZIM-Grant KK5151903BM1), by the European Commission H2020 MCSA Rise (#872488— DCPM) and ERASMUS + people mobility grant (2023-1-ES01-KA131-HED-000120366).

AUTHOR'S STATEMENT

Research funding: As mentioned in the Acknowledgments public funded grants are involved. Conflict of interest: Authors state no conflict of interest. Informed consent: Informed consent has been obtained from all individuals included in this study. Ethical approval: The research related to human use complies with all the relevant national regulations, institutional policies and was performed in accordance with the tenets of the Helsinki Declaration and has been approved by the by the Human Ethics Committee of the University of Canterbury (HEC 2019/01/LR-PS) and the Ethikkommission of the Furtwangen University.

REFERENCES

Ambrisko, T. D., Schramel, J. P., Adler, A., Kutasi, O., Makra, Z., & Moens, Y. P. S. (2016). Assessment of distribution of ventilation by electrical impedance tomography in standing horses. *Physiological Measurement*, *37*(2), 175–186.

Berlin, D. (2012). Hemodynamic Consequences of Auto-PEEP. *29*(2), 81–86.

Cao, X. Y., & Xiao, S. Y. (2018). Chronic lung disease, lung regeneration and future therapeutic strategies. *Chronic Diseases and Translational Medicine*, *4*(2), 103.

Frerichs, I., Amato, M. B. P., Van Kaam, A. H., Tingay, D. G., Zhao, Z., Grychtol, B., Bodenstein, M., Gagnon, H., Böhm, S. H., Teschner, E., Stenqvist, O., Mauri, T., Torsani, V., Camporota, L., Schibler, A., Wolf, G. K., Gommers, D., Leonhardt, S., Adler, A., … Wrigge, H. (2017). Chest electrical impedance tomography examination, data analysis, terminology, clinical use and recommendations: consensus statement of the TRanslational EIT developmeNt stuDy group. *Thorax*, *72*(1), 83–93.

Hochhausen, N., Kapell, T., Dürbaum, M., Follmann, A., Rossaint, R., & Czaplik, M. (2022). Monitoring postoperative lung recovery using electrical impedance tomography in post anesthesia care unit: an observational study. *Journal of Clinical Monitoring and Computing*, *36*(4), 1205–1212.

Krueger-Ziolek, S., Schullcke, B., Kretschmer, J., Müller-Lisse, U., Möller, K., & Zhao, Z. (2015). Positioning of

electrode plane systematically influences EIT imaging. *Physiological Measurement*, *36*(6), 1109–1118.

Laufer, B., Krueger-Ziolek, S., Docherty, P. D., Hoeflinger, F., Reindl, L., & Moeller, K. (2021). An Alternative Way to Measure Tidal Volumes. *IFMBE Proceedings*, *80*, 66–72.

Laufer, B., Murray, R., Docherty, P. D., Krueger-Ziolek, S., Hoeflinger, F., Reindl, L., & Moeller, K. (2020). A Minimal Set of Sensors in a Smart-Shirt to Obtain Respiratory Parameters. *IFAC-PapersOnLine*, *53*(2), 16293–16298.

Lucas, A., Yasa, J., & Lucas, M. (2020). Regeneration and repair in the healing lung. *Clinical & Translational Immunology*, *9*(7).

Massaroni, C., Carraro, E., Vianello, A., Miccinilli, S., Morrone, M., Levai, I. K., Schena, E., Saccomandi, P., Sterzi, S., DIckinson, J. W., Winter, S., & Silvestri, S. (2017). Optoelectronic Plethysmography in Clinical Practice and Research: A Review. *Respiration; International Review of Thoracic Diseases*, *93*(5), 339–354.

Milic-Emili, J., Henderson, J. A., Dolovich, M. B., Trop, D., & Kaneko, K. (1966). Regional distribution of inspired gas in the lung. *Journal of Applied Physiology*, *21*(3), 749–759.

World Health Statistics 2023 - A visual summary. (n.d.). Retrieved January 26, 2024, from https://www.who.int/data/stories/world-health-statistics-2023-a-visual-summary

Yang, L., Dai, M., Cao, X., Möller, K., Dargvainis, M., Frerichs, I., Becher, T., Fu, F., & Zhao, Z. (2021). Regional ventilation distribution in healthy lungs: can reference values be established for electrical impedance tomography parameters? *Annals of Translational Medicine*, *9*(9), 789–789.

Yang, L., Zhao, K., Gao, Z., Fu, F., Wang, H., Wang, C., Dai, J., Liu, Y., Qin, Y., Dai, M., Cao, X., & Zhao, Z. (2023a). The Influence of Breathing Exercises on Regional Ventilation in Healthy and Patients with Chronic Obstructive Pulmonary Disease. *COPD: Journal of Chronic Obstructive Pulmonary Disease*, *20*(1), 248–255.

Yang, L., Zhao, K., Gao, Z., Fu, F., Wang, H., Wang, C., Dai, J., Liu, Y., Qin, Y., Dai, M., Cao, X., & Zhao, Z. (2023b). The Influence of Breathing Exercises on Regional Ventilation in Healthy and Patients with Chronic Obstructive Pulmonary Disease. *COPD: Journal of Chronic Obstructive Pulmonary Disease*, *20*(1), 248–255.

Yang, L., Zhao, K., Gao, Z., Fu, F., Wang, H., Wang, C., Dai, J., Liu, Y., Qin, Y., Dai, M., Cao, X., & Zhao, Z. (2023c). The Influence of Breathing Exercises on Regional Ventilation in Healthy and Patients with Chronic Obstructive Pulmonary Disease. *COPD: Journal of Chronic Obstructive Pulmonary Disease*, *20*(1), 248–255.

Yoshida, T., Piraino, T., Lima, C. A. S., Kavanagh, B. P., Amato, M. B. P., & Brochard, L. (2019). Regional ventilation displayed by electrical impedance tomography as an incentive to decrease positive end-expiratory pressure. *American Journal of Respiratory and Critical Care Medicine*, *200*(7), 933–937.

Zhang, C., Dai, M., Liu, W., Bai, X., Wu, J., Xu, C., Xia, J., Fu, F., Shi, X., Dong, X., Jin, F., & You, F. (2018). Global and regional degree of obstruction determined by electrical impedance tomography in patients with obstructive ventilatory defect. *PLoS ONE*, *13*(12).

Zhou, J. F., & Zhou, J. X. (2021). Lung Volume Measurement. *Respiratory Monitoring in Mechanical Ventilation: Techniques and Applications*, 177–205.

Zick, G., Elke, G., Becher, T., Schädler, D., Pulletz, S., Freitag-Wolf, S., Weiler, N., & Frerichs, I. (2013). Effect of PEEP and Tidal Volume on Ventilation Distribution and End-Expiratory Lung Volume: A Prospective Experimental Animal and Pilot Clinical Study. *PLOS ONE*, *8*(8), e72675.